NONLOCAL PERIMETERS AND CURVATURE FLOWS ON GRAPHS WITH APPLICATIONS IN IMAGE PROCESSING AND HIGH-DIMENSIONAL DATA CLASSIFICATION

Imad El Bouchairi, Abderrahim Elmoataz, Jalal M. Fadili

NONLOCAL PERIMETERS AND CURVATURE FLOWS ON GRAPHS WITH APPLICATIONS IN IMAGE PROCESSING AND HIGH-DIMENSIONAL DATA CLASSIFICATION

IMAD EL BOUCHAIRI*, ABDERRAHIM ELMOATAZ*, AND M. JALAL FADILI*

Abstract. In this paper, we revisit the notion of perimeter on graphs, introduced in [22], and we extend it to so-called inner and outer perimeters. We will also extend the notion of total variation on graphs. Thanks to the co-area formula, we show that discrete total variations can be expressed through these perimeters. Then, we propose a novel class of curvature operators on graphs that unifies both local and nonlocal mean curvature on Euclidean domain. These lead us to translate and adapt the notion of the mean curvature flow on graphs as well as the level set mean curvature, which can be seen as approximate schemes. Finally, we exemplify the usefulness of these methods in image processing, 3D-point cloud and high dimensional data classification.

Key words. Perimeter, total variation, graph cuts, mean curvature flow, image processing, data clustering, PdE on graph, data clustering.

AMS subject classifications. 68Q25, 68R10, 68U05

1. Introduction.

1.1. Context and motivations. Partial Differential Equations (PDEs) and variational methods involving the notion of perimeters and curvatures have and still generate a lot of interest in both continuous and discrete domains. These operators under their different local or nonlocal forms, arise not only from subfields within mathematics such as differential geometry and analysis, but also in numerous PDEs and objective functionals related to many applications fields in sciences and engineering.

For instance, in mathematical image processing and computer vision, the notion of perimeter is a key idea for the regularization of many inverse ill-posed problems such as denoising, restoration, inpainting, segmentation, etc. Regularizing such problems is often used to find suitable clusters among data, to obtain image partitions for segmentation purposes, to denoise or to inpaint images while preserving sharp boundaries. It is worth noting that perimeters appear in the two most popular variational models for image processing and segmentation, namely the total variation and the Mumford-Shah models [15, 40, 37]

Motion by mean curvature and flows involving mean curvature in general play an important role in geometry and analysis. Many continuous models, involving a front propagation with a velocity depending on the mean curvature and their simulations by level set methods, are used in different application fields such as data processing, computer vision, fluid mechanics. For an overview and applications see the books [42, 38, 10] and references therein.

In recent literature, an intense mathematical study has been performed on nonlocal counterpart of the classical perimeters and curvature flows. A notion of fractional perimeters and nonlocal curvature was first introduced by Caffarelli, Roquejoffre and Savin in [11]. The main idea of fractional perimeters is that any point inside an Euclidean set "interact" with any point outside the set, given a functional whose minimization is taken account. Then many works have been proposed to study functional involving nonlocal perimeters or nonlocal curvature flows, e.g [1, 14]. See also the recent monograph Mazon et al. [34]. We can notice that, in the latter, the

*Normandie Univ, ENSICAEN, UNICAEN, CNRS, GREYC, France. E-mail: imad.elbouchairi@gmail.com, abderrahim.elmoataz-billah@unicaen.fr, Jalal.Fadili@ensicaen.fr

authors have introduced a large class of perimeters and curvature flows on random metric graphs which embedded local and nonlocal perimeters on Euclidean domains and graphs [36, 35].

On the other hand, graphs and networks have been successfully used in a variety of fields such as machine learning, data mining, image analysis and social sciences that are confronted with the analysis and modelling high dimensional datasets. In machine learning, image analysis many tasks, such as classification, clustering or segmentation , can be often given in term of minimizing a graph perimeter (graph cut) or a related functional (normalized cut, ratio cut, balanced cut, etc). The cut size is, in this case, generally defined as the sum of the weight of edges between the considered set and its complement, which is closely related to the notion of the perimeter of a set. Such graph problems are traditionally solved by methods from combinatorial, graph theory or spectral analysis [29, 43, 45, 50, 9]. In recent years, there has been increasing interest in applying the models and techniques from variational methods and PDEs to solve problems in data science, see [48, 8, 25, 26] and references herein. The demand and the interest for such methods are motivated by existing and potential future applications in data science. PDEs analysis tools originally developed for Euclidean spaces and regular lattices are now being extended to general settings of graphs in order to analyse geometric and topological structures as well as data measured on them.

In this work, we are going to translate and solved different PDEs on graph. For this purpose, we adopt nonlocal calculus on weighted graphs, see e.g. [25, 23, 26], which consists in replacing continuous partial differential operators (e.g. gradient, divergence), with a reasonable discrete analogue. It allows to transfer many important tools and results from the continuous setting to the discrete one. It also allows graph theory to have new connections to analysis. Based on this framework, we revisit and extend the discrete notions of perimeters, mean curvatures, Cheeger cut and total variation, which lead us to adapt and transcribe level set equations on weighted graphs.

1.2. Outline of the paper. The remainder of the paper is organized as follows. In Section 2 we start by reviewing some basic notations and recalling some preliminary material necessary to our exposition. In Section 3, we revisit the notion of boundary sets on graphs as well as discrete perimeters on graphs. In Section 4, we prove an analogue version of the co-area formula on weighted graphs which allows us to derive relation with discrete p-total variations with discrete perimeters. In Section 5, we introduced a family of the mean curvature flows on graphs. We also propose an adaptation and a transcription of the mean curvature level set equations on general discrete domains, weighted graphs, in Section 6. Finally, we expose some applications in image and data processing to illustrate the potential and the behaviour of this mean curvature formulation.

2. Notations and preliminaries.

2.1. Basics on functions on graphs. A *weighted graph* $G = (V, E, \omega)$ consists of a finite set V of $N \in \mathbb{N}$ vertices, a finite set $E \subseteq V \times V$ of edges, and a weight function $\omega : V \times V \to [0, 1]$. The weight of an edge (u, v) is denoted by ω_{uv}, belongs to the interval $[0, 1]$, and is a measure of similarity between the two vertices. The neighborhood of a vertex u is the set of vertices adjacent to u, and is denoted by $\mathcal{N}(u)$. In the following, we adopt the notation $u \sim v$ to denote two adjacent vertices (i.e., $(u, v) \in E$). The degree $\delta(u)$ of a vertex $u \in V$ is defined as $\delta(u) = \sum_{v \sim u} \sqrt{\omega_{uv}}$.

Throughout this paper, for a subset $\mathcal{A}$ of V, $\mathcal{A}^c$ is its complement, and $\chi_{\mathcal{A}}$ is the characteristic function of $\mathcal{A}$ that taking 1 on $\mathcal{A}$ and 0 otherwise.

Let $G = (V, E, \omega)$ be a weighted graph. We denote by $\mathcal{H}(V)$ the space of real-valued functions on the vertices of G, i.e., each function $f : V \to \mathbb{R}$ in $\mathcal{H}(V)$ assigns a real-value $f(u)$ to each vertex $u \in V$.

For a function $f \in \mathcal{H}(V)$ the $\ell^p(V)$-norm of f is

$$\big\|f\big\|_p = \left(\sum_{u\in V} \big|f(u)\big|^p\right)^{\frac{1}{p}}, \ 1 \leqslant p < \infty, \ \text{ and } \ \big\|f\big\|_\infty = \max_{u\in V} \big|f(u)\big|.$$

The space $\mathcal{H}(V)$ endowed with the inner product: $\langle f, g\rangle_{\mathcal{H}(V)} = \sum_{u\in V} f(u)g(u)$, $f, g \in \mathcal{H}(V)$, is a Hilbert space. Similarly, let $\mathcal{H}(E)$ be the space of real-valued functions defined on the edges of the graph, i.e., each function $H : E \to \mathbb{R}$ in $\mathcal{H}(E)$ assigns a real-valued $H(u, v)$ to each edge $(u, v) \in E$. The space $\mathcal{H}(E)$ endowed with the following inner product: $\langle H, F\rangle_{\mathcal{H}(E)} = \sum_{(u,v)\in E} H(u, v)F(u, v)$, $H, F \in \mathcal{H}(E)$, is a Hilbert space.

2.2. Partial difference operators on graphs. Let us recall some weighted partial difference operators on graphs that are essential in our paper. We refer to [25, 27, 46, 23], for more detailed description of these operators.

The *weighted finite difference operator* of a function $u \in \mathcal{H}(V)$, denoted by $\mathbf{d}_\omega : \mathcal{H}(V) \to \mathcal{H}(E)$, is defined on a pair of vertices $(u, v) \in E$ as:

$$\mathbf{d}_\omega f(u, v) = \sqrt{\omega_{uv}}(f(v) - f(u)).$$

Note that this difference operator is linear and antisymmetric.

The adjoint of the difference operator $\mathbf{d}_\omega$, denoted by $\mathbf{d}^*_\omega : \mathcal{H}(E) \to \mathcal{H}(V)$, is a linear operator, which can be characterized by $\langle \mathbf{d}_\omega f, H\rangle_{\mathcal{H}(E)} = \langle f, \mathbf{d}^*_\omega H\rangle_{\mathcal{H}(V)}$ for all $f \in \mathcal{H}(V)$ and all $H \in \mathcal{H}(E)$. Using the definitions of the finite weighted difference operator and the inner products of $\mathcal{H}(V)$ and $\mathcal{H}(E)$, the adjoint operator $\mathbf{d}^*_\omega$ of a function $H \in \mathcal{H}(E)$ can be expressed at a vertex $u \in V$ by the following expression:

$$\mathbf{d}^*_\omega H(u) = \sum_{v\sim u} \sqrt{\omega_{uv}}(H(v, u) - H(u, v)).$$

The *divergence operator* is defined by

$$\mathbf{div}_\omega = -\mathbf{d}^*_\omega,$$

measures the net outflow of a function of $\mathcal{H}(E)$ at each vertex of the graph. Each function $H \in \mathcal{H}(E)$ has a null divergence over the entire set of vertices. Indeed, from the previous definitions, it can be easily shown that $\sum_{u\in V}\sum_{v\sim u} \mathbf{d}_\omega f(u, v) = 0$, for all $f \in \mathcal{H}(V)$, and $\sum_{u\in V} \mathbf{div}_\omega H(u) = 0$, for all $H \in \mathcal{H}(E)$.

The *weighted directional finite difference* of f at a vertex u along the edge (u, v) is defined as:

$$\partial_v f(u) = \sqrt{\omega_{uv}}(f(v) - f(u)).$$

Similarly we define the upwind and downwind weighted directional finite differences of f at a vertex u along the edge (u, v) as:

$$\partial^\pm_v f(u) = \sqrt{\omega_{uv}}\,(f(v) - f(u))^\pm,$$

where $a^+ = \max(a, 0)$ and $a^- = \max(-a, 0)$, $a \in \mathbb{R}$. Based on these definitions, we introduce the *weighted gradient* operator on graphs $\nabla_\omega : \mathcal{H}(V) \to \mathcal{H}(V)$, which is defined on a vertex $u \in V$ as the vector of all weighted finite differences with respect to the set of vertices V, that is

$$(\nabla_\omega f)(u) = (\partial_v f(u))_{v \in V}.$$

From the properties of the weighted partial difference operators, it gets clear that the weighted gradient is linear and antisymmetric. Similarly we define the upwind downwind weighted gradient operators on graphs $\nabla_\omega^\pm : \mathcal{H}(V) \to \mathcal{H}(V)$

$$(\nabla_\omega^\pm f)(u) = (\partial_v^\pm f(u))_{v \in V}, \text{ for all } u \in V.$$

A family of gradient norms $\|\cdot\|_p \circ \nabla_\omega$, $\|\cdot\|_p \circ \nabla_\omega^\pm : \mathcal{H}(V) \to (\mathbb{R}^+)^{|V|}$ with $1 \leqslant p \leqslant \infty$ is given as:

$$\begin{aligned} \big\|(\nabla_\omega f)(u)\big\|_p &= \left(\sum_{v \sim u} (\omega_{uv})^{\frac{p}{2}} \big|f(v) - f(u)\big|^p\right)^{\frac{1}{p}}, \quad 1 \leqslant p < \infty \\ \big\|(\nabla_\omega f)(u)\big\|_\infty &= \max_{v \sim u} (\sqrt{\omega_{uv}} \big|f(v) - f(u)\big|) \end{aligned}$$

and likewise for the operator $\nabla_\omega^\pm$ instead of ∇_ω. The integral of a function f in $\mathcal{H}(V)$ (with respect to the empirical measure on V) is defined by:

$$E(f) = \sum_{u \in V} f(u).$$

p-Laplacians Using the difference and the divergence operators, as in the continuous settings, the p-Laplacian operator for $1 \leq p < \infty$) is

$$(\Delta_{\omega,2} f)(u) = \frac{1}{2} \mathbf{div}_\omega \left(|\mathbf{d}_\omega f|^{p-2} \cdot \mathbf{d}_\omega f\right)(u).$$

By developing we equivalently obtain

$$(\Delta_{\omega,2} f)(u) = \sum_{v \in V} \omega_{uv}^{\frac{p}{2}} \big|f(v) - f(u)\big|^{p-2} (f(v) - f(u)).$$

Notable particular cases are:

$$p = 2: \quad (\Delta_{\omega,2} f)(u) = \sum_{u \in V} \omega_{uv} (f(v) - f(u)) \qquad \text{which is the Laplacian,}$$

$$p = 1: \quad (\Delta_{\omega,1} f)(u) = \sum_{u \in V} \sqrt{\omega_{uv}} \frac{f(v) - f(u)}{\big|f(v) - f(u)\big|} \qquad \text{which is the 1-Laplacian.}$$

The graph p-Laplacian have been used as a discretization of the continuous local and nonlocal p-Laplacian see [20, 13] and [28, 21], respectively.

The ∞-Laplacian on graphs is defined by

$$(\Delta_{\omega,\infty} f)(u) = \frac{1}{2} \left(\big\|\nabla_\omega^+ f(u)\big\|_\infty - \big\|\nabla_\omega^- f(u)\big\|_\infty\right).$$

Game p-Laplacians Based on the above definition of the p-Laplacian, the game p-Laplacian is given as follows

$$(\Delta^G_{\omega,p} f)(u) = \begin{cases} \frac{2}{p}(\Delta_{\omega,2} f)(u) + \frac{p-2}{p}(\Delta_{\omega,\infty} f)(u), & \text{for } 2 \le p \le \infty, \\ \frac{2(p-1)}{p}(\Delta_{\omega,2} f)(u) + \frac{2-p}{p}(\Delta_{\omega,1} f)(u), & \text{for } 1 \le p \le 2. \end{cases} \tag{2.1}$$

See [24] for more details. Observe that the game p-Laplacian can be interpreted as discrete version of the continuous game p-Laplacian, [39].

3. Generalized perimeters on graphs.

3.1. Boundaries on graphs.

We start by defining the notion of boundaries on graphs

DEFINITION 3.1. *The* outer *and* inner vertex boundaries*, and the* vertex boundary*, of a subset $\mathcal{A} \subset V$, are respectively defined by:*

$$\partial^+ \mathcal{A} \stackrel{\text{def}}{=} \{u \in \mathcal{A}^c : \exists v \in \mathcal{A},\, v \sim u\}, \tag{3.1}$$

$$\partial^- \mathcal{A} \stackrel{\text{def}}{=} \{u \in \mathcal{A} : \exists v \in \mathcal{A}^c,\, v \sim u\}, \tag{3.2}$$

$$\partial \mathcal{A} \stackrel{\text{def}}{=} \partial^+ \mathcal{A} \cup \partial^- \mathcal{A}. \tag{3.3}$$

Note that $\partial^+ \mathcal{A}^c = \partial^- \mathcal{A}$, $\partial \mathcal{A} = \partial \mathcal{A}^c$ and $\partial^+ \mathcal{A} \cap \partial^- \mathcal{A} = \emptyset$.

The following proposition gives relationships between the discrete gradients and the above boundary sets, which will be useful to define the discrete perimeters on graphs. The proof is a simple computation of the p-norm of the characteristic function and we omit here for the sake of brevity.

PROPOSITION 3.1. *Let $\mathcal{A} \subset V$,*

(i) For $1 \le p < \infty$, we have the following relations:

$$\|(\nabla^+_\omega \chi_{\mathcal{A}})(u)\|_p = \left(\sum_{v \in \mathcal{A}} (\omega_{uv})^{\frac{p}{2}} \right)^{\frac{1}{p}} \chi_{\partial^+ \mathcal{A}}(u), \tag{3.4}$$

$$\left\|(\nabla^-_\omega \chi_{\mathcal{A}})(u)\right\|_p = \left(\sum_{v \in \mathcal{A}^c} (\omega_{uv})^{\frac{p}{2}} \right)^{\frac{1}{p}} \chi_{\partial^- \mathcal{A}}(u), \tag{3.5}$$

$$\left\|(\nabla_\omega \chi_{\mathcal{A}})(u)\right\|_p = \left\|(\nabla^+_\omega \chi_{\mathcal{A}})(u)\right\|_p + \left\|(\nabla^-_\omega \chi_{\mathcal{A}})(u)\right\|_p. \tag{3.6}$$

(ii) For $p = \infty$, we have the following relations:

$$\|(\nabla^+_\omega \chi_{\mathcal{A}})(u)\|_\infty = \left(\max_{v \in \mathcal{A}} (\sqrt{\omega_{uv}}) \right) \cdot \chi_{\partial^+ \mathcal{A}}(u),$$

$$\left\|(\nabla^-_\omega \chi_{\mathcal{A}})(u)\right\|_\infty = \left(\max_{v \in \mathcal{A}^c} (\sqrt{\omega_{uv}}) \right) \cdot \chi_{\partial^- \mathcal{A}}(u),$$

$$\left\|(\nabla_\omega \chi_{\mathcal{A}})(u)\right\|_\infty = \left\|(\nabla^+_\omega \chi_{\mathcal{A}})(u)\right\|_\infty + \left\|(\nabla^-_\omega \chi_{\mathcal{A}})(u)\right\|_\infty.$$

(iii) For $p \in [1, +\infty]$, we have the following relations:

$$\left\|(\nabla^+_\omega \chi_{\mathcal{A}})(u)\right\|_p = \left\|(\nabla^-_\omega \chi_{\mathcal{A}^c})(u)\right\|_p$$

$$\left\|(\nabla_\omega \chi_{\mathcal{A}})(u)\right\|_p = \left\|(\nabla_\omega \chi_{\mathcal{A}^c})(u)\right\|_p.$$

REMARK 3.1. *For unweighted graphs i.e. $\omega_{uv} \in \{0, 1\}$, we have that:*

- $\|(\nabla_\omega^+ \chi_{\mathcal{A}})(u)\|_1$ *corresponds to the number of edges connecting the vertex* $u \in \mathcal{A}^c$ *with the vertices in* $\mathcal{A}$. *Therefore* $\sum_{u\in V} \left\|(\nabla_\omega^+ \chi_{\mathcal{A}})(u)\right\|_1$ *is just the size of the usual edge boundary of* $\mathcal{A}$.
- $\|(\nabla_\omega^+ \chi_{\mathcal{A}})(u)\|_\infty$ *is the indicator of* $\partial^+\mathcal{A}$, *and so* $\sum_{u\in V} \left\|(\nabla_\omega^+ \chi_{\mathcal{A}})(u)\right\|_\infty$ *is the size of the outer vertex boundary of* $\mathcal{A}$, *while* $\sum_{u\in V} \left\|(\nabla_\omega^- \chi_{\mathcal{A}})(u)\right\|_\infty$ *is the size of the inner vertex boundary.*

For weighted graphs i.e. $\omega_{uv} \in [0,1]$, *we observe that:*

- $\|(\nabla_\omega^+ \chi_{\mathcal{A}})(u)\|_p$ *and* $\left\|(\nabla_\omega^- \chi_{\mathcal{A}})(u)\right\|_p$ *are the weighted sizes of edge boundaries of* $\mathcal{A}$ *for* $\partial^+\mathcal{A} \times \partial^-\mathcal{A}$ *and* $\partial^-\mathcal{A} \times \partial^+\mathcal{A}$ *respectively.*
- $\sum_{u\in V} \left\|(\nabla_\omega^+ \chi_{\mathcal{A}})(u)\right\|_\infty$ *is the weighted size of the outer vertex boundary of* $\mathcal{A}$ *while* $\sum_{u\in V} \left\|(\nabla_\omega^- \chi_{\mathcal{A}})(u)\right\|_\infty$ *is the weighted size of the inner vertex boundary of* $\mathcal{A}$.

REMARK 3.2. *The* outer *and* inner vertex boundaries, *and the* vertex boundary *can be expressed through the characteristic function of* $\mathcal{A}$ *as:*

$$\partial^+\mathcal{A} = \left\{u \in V : \ \left\|(\nabla_\omega^+ \chi_{\mathcal{A}})(u)\right\|_p > 0\right\},$$

$$\partial^-\mathcal{A} = \left\{u \in V : \ \left\|(\nabla_\omega^- \chi_{\mathcal{A}})(u)\right\|_p > 0\right\},$$

$$\partial\mathcal{A} = \left\{u \in V : \ \left\|(\nabla_\omega \chi_{\mathcal{A}})(u)\right\|_p > 0\right\}.$$

3.2. Discrete perimeters on graphs. Based on the interpretation of Proposition 3.1, we recall the definition of the family of weighted perimeters on graphs introduced in [22].

DEFINITION 3.2. *For* $1 \le p < \infty$ *and* $\mathcal{A} \subset V$, *the family of weighted perimeters of* $\mathcal{A}$ *is defined as follows:*

$$\mathrm{Per}_{\omega,p}^+(\mathcal{A}) \stackrel{\text{def}}{=} E(\left\|\nabla_w^+ \chi_{\mathcal{A}}\right\|_p) = \sum_{u\in\mathcal{A}^c} \left(\sum_{v\in\mathcal{A}} \omega_{uv}^{\frac{p}{2}}\right)^{\frac{1}{p}},$$

$$\mathrm{Per}_{\omega,p}^-(\mathcal{A}) \stackrel{\text{def}}{=} E(\left\|\nabla_\omega^- \chi_{\mathcal{A}}\right\|_p) = \sum_{u\in\mathcal{A}} \left(\sum_{v\in\mathcal{A}^c} \omega_{uv}^{\frac{p}{2}}\right)^{\frac{1}{p}},$$

$$\mathrm{Per}_{\omega,p}(\mathcal{A}) \stackrel{\text{def}}{=} E(\left\|\nabla_\omega \chi_{\mathcal{A}}\right\|_p) = \sum_{u\in\mathcal{A}^c} \left(\sum_{v\in\mathcal{A}} \omega_{uv}^{\frac{p}{2}}\right)^{\frac{1}{p}} + \sum_{u\in\mathcal{A}} \left(\sum_{v\in\mathcal{A}^c} \omega_{uv}^{\frac{p}{2}}\right)^{\frac{1}{p}}.$$

For $p = \infty$, *the family of weighted perimeters of* $\mathcal{A}$ *is defined as follows:*

$$\mathrm{Per}_{\omega,\infty}^+(\mathcal{A}) \stackrel{\text{def}}{=} E(\left\|\nabla_\omega^+ \chi_{\mathcal{A}}\right\|_\infty) = \sum_{u\in\mathcal{A}^c} \left(\max_{v\in\mathcal{A}} \sqrt{\omega_{uv}}\right),$$

$$\mathrm{Per}_{\omega,\infty}^-(\mathcal{A}) \stackrel{\text{def}}{=} E(\left\|\nabla_\omega^- \chi_{\mathcal{A}}\right\|_\infty) = \sum_{u\in\mathcal{A}} \left(\max_{v\in\mathcal{A}^c} \sqrt{\omega_{uv}}\right),$$

$$\mathrm{Per}_{\omega,\infty}(\mathcal{A}) \stackrel{\text{def}}{=} E(\left\|\nabla_\omega \chi_{\mathcal{A}}\right\|_\infty) = \sum_{u\in\mathcal{A}^c} \left(\max_{v\in\mathcal{A}} \sqrt{\omega_{uv}}\right) + \sum_{u\in\mathcal{A}} \left(\max_{v\in\mathcal{A}^c} \sqrt{\omega_{uv}}\right).$$

By definition we have, for $1 \leq p \leq \infty$, the following relations:

$$\begin{aligned}
\mathrm{Per}_{\omega,p}(\mathcal{A}) &= \mathrm{Per}^{+}_{\omega,p}(\mathcal{A}) + \mathrm{Per}^{-}_{\omega,p}(A),\\
\mathrm{Per}^{+}_{\omega,p}(\mathcal{A}) &= \mathrm{Per}^{-}_{\omega,p}(\mathcal{A}^c),\\
\mathrm{Per}_{\omega,p}(\mathcal{A}) &= \mathrm{Per}_{\omega,p}(\mathcal{A}^c),\\
\mathrm{Per}_{\omega,1}(\mathcal{A}) &= 2\,\mathrm{Per}^{+}_{\omega,1}(\mathcal{A}).
\end{aligned}$$

PROPOSITION 3.2. *Let P_ω belongs to $\{\mathrm{Per}^{\pm}_{\omega,1},\ \mathrm{Per}^{\pm}_{\omega,\infty},;\mathrm{Per}_{\omega,1},\ \mathrm{Per}_{\omega,\infty}\}$. In the case $p=\infty$, we asume that the weight function ω is a $\{0,1\}$-value. We have the following properties:*

(i) $P_\omega(\emptyset) = 0$;

(ii) $P_\omega(V) = 0$;

(iii) P_ω *is submodular, i.e. for all* $\mathcal{A},\ \mathcal{B} \subset V$ *we have*

$$P_\omega(\mathcal{A}\cup\mathcal{B}) + P_\omega(\mathcal{A}\cap\mathcal{B}) \leq P_\omega(\mathcal{A}) + P_\omega(\mathcal{B}).$$

PROOF : Claims (i) and (ii) are straightforward. We thus focus on claim (iii). For $p=1$, it is enough to prove the inequality for $\mathrm{Per}^{+}_{\omega,1}$ since $\mathrm{Per}_{\omega,1} = 2\,\mathrm{Per}^{+}_{\omega,1} = 2\,\mathrm{Per}^{+}_{\omega,1}$. We have

$$\begin{aligned}
\mathrm{Per}^{+}_{\omega,1}(\mathcal{A}\cup\mathcal{B}) &= \sum_{u\in\mathcal{A}\cup\mathcal{B}}\sum_{v\in(\mathcal{A}\cup\mathcal{B})^c}\sqrt{\omega_{uv}}\\
&= \sum_{u\in\mathcal{A}}\sum_{v\in\mathcal{A}^c}\sqrt{\omega_{uv}} + \sum_{u\in\mathcal{B}}\sum_{v\in\mathcal{B}^c}\sqrt{\omega_{uv}} - \sum_{u\in\mathcal{A}\cap\mathcal{B}}\sum_{v}\in(\mathcal{A}\cup\mathcal{B})^c\sqrt{\omega_{uv}}\\
&\quad - \sum_{u\in\mathcal{A}}\sum_{v\in\mathcal{B}\setminus(\mathcal{A}\cup\mathcal{B})^c}\sqrt{\omega_{uv}} - \sum_{u\in\mathcal{B}}\sum_{v\in\mathcal{A}\setminus(\mathcal{A}\cup\mathcal{B})^c}\sqrt{\omega_{uv}},
\end{aligned}$$

and

$$\begin{aligned}
\mathrm{Per}^{+}_{\omega,1}(\mathcal{A}\cap\mathcal{B}) &= \sum_{u\in\mathcal{A}\cap\mathcal{B}}\sum_{v\in(\mathcal{A}\cap\mathcal{B})^c}\sqrt{\omega_{uv}}\\
&= \sum_{u\in\mathcal{A}\cap\mathcal{B}}\sum_{v\in(\mathcal{A}\cup\mathcal{B})^c}\sqrt{\omega_{uv}} + \sum_{u\in\mathcal{A}\cap\mathcal{B}}\sum_{v\in\mathcal{A}\setminus(\mathcal{A}\cup\mathcal{B})^c}\sqrt{\omega_{uv}}\\
&\quad + \sum_{u\in\mathcal{A}\cap\mathcal{B}}\sum_{v\in\mathcal{B}\setminus(\mathcal{A}\cup\mathcal{B})^c}\sqrt{\omega_{uv}}.
\end{aligned}$$

For $\mathrm{Per}^{\pm}_{\omega,\infty}$, claim (iii) is a consequence of the following inequality, which is easy to verify,

$$\begin{aligned}
&\max_{v\sim u}\left(\chi_{\mathcal{A}\cup\mathcal{B}}(v) - \chi_{\mathcal{A}\cup\mathcal{B}}(u)\right)^{\pm} + \max_{v\sim u}\left(\chi_{\mathcal{A}\cap\mathcal{B}}(v) - \chi_{\mathcal{A}\cap\mathcal{B}}(u)\right)^{\pm}\\
&\qquad\leq \max_{v\sim u}\left(\chi_{\mathcal{A}}(v) - \chi_{\mathcal{A}}(u)\right)^{\pm} + \max_{v\sim u}\left(\chi_{\mathcal{B}}(v) - \chi_{\mathcal{B}}(u)\right)^{\pm},
\end{aligned}$$

for all $u \in V$. For $\mathrm{Per}_{\omega,\infty}$, the result holds from the following equality $\mathrm{Per}_{\omega,\infty} = \mathrm{Per}^{+}_{\omega,\infty} + \mathrm{Per}^{-}_{\omega,\infty}$. □

As a consequence, we have the following result for $p=1$.

COROLLARY 3.1. *Let $\mathcal{A},\ \mathcal{B} \subset V$ with $\mathcal{A}\cap\mathcal{B} = \emptyset$, then*

$$\mathrm{Per}^{\pm}_{\omega,1}(\mathcal{A}\cup\mathcal{B}) = \mathrm{Per}^{\pm}_{\omega,1}(\mathcal{A}) + \mathrm{Per}^{\pm}_{\omega,1}(\mathcal{B}) - 2\sum_{\mathcal{A}}\sum_{\mathcal{B}}\sqrt{\omega_{uv}},$$

$$\mathrm{Per}_{\omega,1}(\mathcal{A}\cup\mathcal{B}) = \mathrm{Per}_{\omega,1}(\mathcal{A}) + \mathrm{Per}_{\omega,1}(\mathcal{B}) - 4\sum_{\mathcal{A}}\sum_{\mathcal{B}}\sqrt{\omega_{uv}}.$$

If moreover, there are no edges between $\mathcal{A}$ and $\mathcal{B}$, i.e., $\partial\mathcal{A}\cap\mathcal{B}=\emptyset$ or equivalently $\partial\mathcal{B}\cap\mathcal{A}=\emptyset$, then

$$\mathrm{Per}^{\pm}_{\omega,1}(\mathcal{A}\cup\mathcal{B}) = \mathrm{Per}^{\pm}_{\omega,1}(\mathcal{A}) + \mathrm{Per}^{\pm}_{\omega,1}(\mathcal{B}),$$
$$\mathrm{Per}_{\omega,1}(\mathcal{A}\cup\mathcal{B}) = \mathrm{Per}_{\omega,1}(\mathcal{A}) + \mathrm{Per}_{\omega,1}(\mathcal{B}).$$

Proof : By definition, we have

$$\begin{aligned}
\mathrm{Per}_{\omega,1}(\mathcal{A}\cup\mathcal{B}) &= \sum_{u\in V}\sum_{v\in V}\sqrt{\omega_{uv}}\left(\chi_{\mathcal{A}\cup\mathcal{B}}(v)-\chi_{\mathcal{A}\cup\mathcal{B}}(u)\right)^2\\
&= \sum_{u\in V}\sum_{v\in V}\sqrt{\omega_{uv}}\left(\chi_{\mathcal{A}}(v)+\chi_{\mathcal{B}}(v)-\chi_{\mathcal{A}}(u)-\chi_{\mathcal{B}}(u)\right)^2\\
&= \sum_{u\in V}\sum_{v\in V}\sqrt{\omega_{uv}}\left(\chi_{\mathcal{A}}(v)-\chi_{\mathcal{A}}(u)\right)^2 + \sum_{u\in V}\sum_{v\in V}\sqrt{\omega_{uv}}\left(\chi_{\mathcal{B}}(v)-\chi_{\mathcal{B}}(u)\right)^2\\
&\qquad + 2\cdot\sum_{u\in V}\sum_{v\in V}\sqrt{\omega_{uv}}\left(\chi_{\mathcal{A}}(v)-\chi_{\mathcal{A}}(u)\right)\cdot\left(\chi_{\mathcal{B}}(v)-\chi_{\mathcal{B}}(u)\right)\\
&= \mathrm{Per}_{\omega,1}(\mathcal{A}) + \mathrm{Per}_{\omega,1}(\mathcal{B}) - 4\cdot\sum_{\mathcal{A}}\sum_{\mathcal{B}}\sqrt{\omega_{uv}}.
\end{aligned}$$

We obtain the result for $\mathrm{Per}^{\pm}_{\omega,1}$ immediately from the following relation $\mathrm{Per}^{\pm}_{\omega,1} = \frac{1}{2}\mathrm{Per}_{\omega,1}$. □

Remark 3.3. *The notion of nonlocal perimeter was introduced in [5, 17] and was thoroughly studied in [7, 34]. For the singular kernels, we recall the nonlocal s-perimeter, $s\in]0,1[$, which is given for a subset $\mathcal{A}\subset\mathbb{R}^n$ as*

$$\mathrm{Per}_s(\mathcal{A}) = \int_{\mathcal{A}}\int_{\mathcal{A}^c}\frac{1}{\left|\boldsymbol{x}-\boldsymbol{y}\right|^{n+s}}d\boldsymbol{y}d\boldsymbol{x}.$$

It has been proven that the usuel notion of perimeter is recovered by the limit

$$\lim_{s\to 1}(1-s)\,\mathrm{Per}_s(\mathcal{A}) = \mathrm{Per}(\mathcal{A}) = \int_{\mathbb{R}^N}\left|D\chi_{\mathcal{A}}\right|,$$

see [4, 7, 12, 17].
In turn, we will show that the definition of the (s-)perimeter can be recovered by our definition, as the number of the vertices goes to infinity. Indeed, set $J:\boldsymbol{x}\mapsto\frac{1}{|\boldsymbol{x}|^{n+s}}$, and let $\{J_k\}_k$ be a sequence of symmetric positive functions in $L^1(\mathbb{R}^n)$ satisfying:

(i) *for all k, J_k of compact support and $J_k = \sum_{\boldsymbol{x}\in\frac{1}{k}\mathbb{Z}^n}\alpha_{\boldsymbol{x}}\chi_{Q^k_{\boldsymbol{x}}}$, where $\alpha_{\boldsymbol{x}}\in\mathbb{R}^+$ and $Q^k_{\boldsymbol{x}} = \boldsymbol{x}+\frac{1}{k^n}[0,1[^n$.*

(ii) *$\{J_k\}_k$ converges to J strongly in $L^1(\mathbb{R}^n)$.*

Fix $k\in\mathbb{N}^\star$. Consider $G_k=(V_k,E_k,\omega_k)$ where $V_k=\frac{1}{k}\mathbb{Z}^n$ and the weight function is given $\omega_k(\boldsymbol{x},\boldsymbol{y}) = (k^{2n}J_k(\boldsymbol{x}-\boldsymbol{y}))^2$, $\forall\,\boldsymbol{x},\boldsymbol{y}\in V_k$. For all $\mathcal{A}\subset\mathbb{R}^n$, we set $\mathcal{A}^d_k = \left\{\boldsymbol{x}\in V_k:\ Q^k_{\boldsymbol{x}}\cap\mathcal{A}\neq\emptyset\right\}$ and $\mathcal{A}_k = \bigcup_{\boldsymbol{x}\in\mathcal{A}^d_k}Q^k_{\boldsymbol{x}}$. Then

$$\mathrm{Per}_{\omega_k,1}(\mathcal{A}^d_k) = \sum_{\boldsymbol{y}\in\mathcal{A}^d_k}\sum_{\boldsymbol{x}\in(\mathcal{A}^d_k)^c}\sqrt{\omega_k(\boldsymbol{x},\boldsymbol{y})} = \int_{\mathcal{A}_k}\int_{(\mathcal{A}_k)^c}J_k(\boldsymbol{x}-\boldsymbol{y})d\boldsymbol{x}d\boldsymbol{y}.$$

By construction, we can easy check that

$$\lim_k \int_{\mathcal{A}_k}\int_{(\mathcal{A}_k)^c} J_k(\boldsymbol{x}-\boldsymbol{y})d\boldsymbol{x}d\boldsymbol{y} = \int_{\mathcal{A}}\int_{\mathcal{A}^c} J(\boldsymbol{x}-\boldsymbol{y})d\boldsymbol{x}d\boldsymbol{y}.$$

Hence

$$\begin{aligned}\lim_k \mathrm{Per}_{\omega_k,1}(\mathcal{A}_k^d) &= \int_{\mathcal{A}}\int_{\mathcal{A}^c} J(\boldsymbol{x}-\boldsymbol{y})d\boldsymbol{x}d\boldsymbol{y}\\ &= \mathrm{Per}_s(\mathcal{A}).\end{aligned}$$

4. Generalized total variation on graphs. In this section, we extend the notion of total variation, for $p = 1$, on graphs to upwind and downwind p-total variations and also for $p \in [1,\infty]$. We show that the result of the co-area formula provided in [22, 48] is still valid for $p = \infty$ on unweighted graphs.

DEFINITION 4.1. *For $1 \le p < \infty$, the p-total variation on graphs is defined as follows:*

$$\mathrm{TV}_{\omega,p}(f) = E\left(\left\|\nabla_\omega f\right\|_p\right) = \sum_{u\in V}\left(\sum_{v\in V}\omega_{uv}^{\frac{p}{2}}\left|f(v)-f(u)\right|^p\right)^{\frac{1}{p}}$$

$$\mathrm{TV}^{\pm}_{\omega,p}(f) = E\left(\left\|\nabla^{\pm}_\omega f\right\|_p\right) = \sum_{u\in V}\left(\sum_{v\in V}\omega_{uv}^{\frac{p}{2}}\left((f(v)-f(u))^{\pm}\right)^p\right)^{\frac{1}{p}}.$$

Similarly we define the ∞-total variations for $p = \infty$:

$$\mathrm{TV}_{\omega,\infty}(f) = E\left(\left\|\nabla_\omega f\right\|_\infty\right) = \sum_{u\in V}\left(\max_{v\in V}\sqrt{\omega_{uv}}\left|f(v)-f(u)\right|\right)$$

$$\mathrm{TV}^{\pm}_{\omega,\infty}(f) = E\left(\left\|\nabla^{\pm}_\omega f\right\|_\infty\right) = \sum_{u\in V}\left(\max_{v\in V}\sqrt{\omega_{uv}}(f(v)-f(u))^{\pm}\right).$$

It is known that in the continuous case that the perimeter is linked to the total variation via co-area formula. A similar results have been exposed in [22, 48] for the discrete case. For the reader's convenience, we recall this result and their extension to the upwind and downwind p-total variations, for $p \in \{1,\infty\}$.

PROPOSITION 4.1. *For any function $f : V \to \mathbb{R}$, we have:*

$$\mathrm{TV}^{\pm}_{\omega,1}(f) = \int_{-\infty}^{+\infty}\mathrm{TV}^{\pm}_{\omega,1}(\chi_{\{f>t\}})dt, \tag{4.1}$$

$$\mathrm{TV}_{\omega,1}(f) = \int_{-\infty}^{+\infty}\mathrm{TV}_{\omega,1}(\chi_{\{f>t\}})dt. \tag{4.2}$$

In particular, for all $\mathcal{A} \subset V$ we have

$$\mathrm{TV}^{\pm}_{\omega,1}(\chi_{\mathcal{A}}) = \mathrm{Per}^{\pm}_{\omega,1}(\mathcal{A}) \text{ and } \mathrm{TV}_{\omega,1}(\chi_{\mathcal{A}}) = \mathrm{Per}_{\omega,1}(\mathcal{A}).$$

PROOF : See [48] for a detailed proof of (4.2). The proof of (4.1) holds from (4.2) and the following relationship:

$$\mathrm{TV}^{\pm}_{\omega,1}(f) = \frac{1}{2}\mathrm{TV}_{\omega,1}(f), \text{ for every function } f \in \mathcal{H}(V).$$

□

For $p = \infty$, the co-area formula holds for unweighted graphs, as the following proposition shows. To remove confusion on the notation, we denote $\omega = 1$ to signify that the considered graph is unweighted.

PROPOSITION 4.2. *For any function $f : V \to \mathbb{R}$, we have:*

$$\mathrm{TV}^{\pm}_{\omega=1,\infty}(f) = \int_{-\infty}^{+\infty} \mathrm{TV}^{\pm}_{\omega=1,\infty}(\chi_{\{f>t\}})dt,$$

$$\mathrm{TV}_{\omega=1,\infty}(f) = \int_{-\infty}^{+\infty} \mathrm{TV}_{\omega=1,\infty}(\chi_{\{f>t\}})dt.$$

PROOF : Let $u \in V$ and let $v_u \in \mathcal{N}(u)$ such that $\left\|\nabla^{\pm}_{\omega=1} f(u)\right\|_{\infty} = (f(v_u) - f(u))^{\pm}$, we can easy to see that $\left\|\nabla^{\pm}_{\omega=1}\chi_{\{f>t\}}(u)\right\|_{\infty} = \left(\chi_{\{f>t\}}(v_u) - \chi_{\{f>t\}}(u)\right)^{\pm}$ for all $t \in \mathbb{R}$. Then

$$\begin{aligned}
\|\nabla^{\pm}_{\omega=1} f(u)\|_{\infty} &= (f(v_u) - f(u))^{\pm} \\
&= \int_{-\infty}^{+\infty} \left(\chi_{\{f>t\}}(v_u) - \chi_{\{f>t\}}(u)\right)^{\pm} dt \\
&= \int_{-\infty}^{+\infty} \|\nabla^{\pm}_{\omega=1}\chi_{\{f>t\}}(u)\|_{\infty} dt
\end{aligned}$$

Hence,

$$\mathrm{TV}^{\pm}_{\omega=1,\infty}(f) = \int_{-\infty}^{+\infty} E\left(\left\|\nabla^{\pm}_{\omega=1}\chi_{\{f>t\}}\right\|_{\infty}\right) dt = \int_{-\infty}^{+\infty} \mathrm{TV}^{\pm}_{\omega=1,\infty}(\chi_{\{f>t\}})dt.$$

Using the fact that $\mathrm{TV}_{\omega=1,\infty}(f) = \mathrm{TV}^{+}_{\omega=1,\infty}(f) + \mathrm{TV}^{-}_{\omega=1,\infty}(f)$, one gets the last equality. □

REMARK 4.1. *For $p = \infty$, the co-area formula doesn't hold for a general weighted graphs. Indeed, let G be a weighted graph with the vertex set $V = \{1, 2, 3\}$ and the weight function is given by*

$$\omega^2_{ij} = \begin{cases} 1, & \text{if } (i,j) = (1,2), \\ 1/4, & \text{if } (i,j) = (1,3), \\ 1/3, & \text{if } (i,j) = (2,3). \end{cases}$$

Consider the following function defined on V by $f(1) = 0$, $f(2) = 1$, $f(3) = 4$. By a simple computations one gets that

$$\mathrm{TV}^{\pm}_{\omega,\infty}(f) = 2 < \frac{11}{4} = \int_{-\infty}^{+\infty} \mathrm{TV}^{\pm}_{\omega,\infty}(\chi_{\{f>t\}})dt,$$

$$\mathrm{TV}_{\omega,\infty}(f) = 3 < 5 = \int_{-\infty}^{+\infty} \mathrm{TV}_{\omega,\infty}(\chi_{\{f>t\}})dt.$$

We close this subsection with an application of co-area formulas to an equivalent result on functional inequalities.

Let $\mathcal{G}$ be a non-empty set of pairs (g_1, g_2) functions on V an let $\mathcal{L}$ be a functional generated by $\mathcal{G}$ as follow:

$$\mathcal{L}(f) = \sup_{(g_1,g_2)\in\mathcal{G}} E(f^+ g_1 + f^- g_2). \tag{4.3}$$

We say that the functional $\mathcal{L}$ admits a quasi-linear representations. As noted in [47], many functionals have this representation, for example:

$$\mathcal{L}(f) = \left(E\left(\left|f\right|^p\right)\right)^{1/p}, \text{ for } 1 \le p \le \infty,$$
$$\mathcal{L}(f) = \left(E\left(\left|f - E(f)\right|^p\right)\right)^{1/p}, \text{ for } 1 \le p \le \infty,$$
$$\mathcal{L}(f) = \inf_{a\in\mathbb{R}} \left(E\left(\left|f - a\right|^p\right)\right)^{1/p} \text{ for } 1 \le p \le \infty.$$

The co-area formula implies the following equivalence.

PROPOSITION 4.3. *Let $\lambda > 0$, and either $p = 1$ or $p = \infty$ with $\omega \in \{0, 1\}$, the following are equivalent:*

(i) $\mathcal{L}(f) \le \lambda E(\left\|\nabla^{\pm}_{\omega} f\right\|_p)$ *for all* $f : V \to \mathbb{R}$.

(ii) $\mathcal{L}(\chi_{\mathcal{A}}) \le \lambda E(\left\|\nabla^{\pm}_{\omega} \chi_{\mathcal{A}}\right\|_p)$ *and* $\mathcal{L}(-\chi_{\mathcal{A}}) \le \lambda E(\left\|\nabla^{\pm}_{\omega}(-\chi_{\mathcal{A}})\right\|_p)$, *for all* $\mathcal{A} \subset V$.

PROOF : The implication (i) $\Longrightarrow$ (ii) is straightforward, it is enough to apply (i) to $f = \chi_A$ and $f = -\chi_{\mathcal{A}}$. Conversely, let $g_1, g_2 \in \mathcal{G}$, it is easy to see $E(\left\|\nabla^{\pm}_{\omega} \chi_{\mathcal{A}}\right\|_p) = E(\left\|\nabla^{\pm}_{\omega} \left(-\chi_{\mathcal{A}^c}\right)\right\|_p)$ for all $\mathcal{A} \subset V$. Therefore

$$\begin{aligned} E(\left\|\nabla^{\pm}_{\omega} f\right\|_p) &= \int_0^{+\infty} E(\left\|\nabla^{\pm}_{\omega} \chi_{\{f>t\}}\right\|_p)dt + \int_{-\infty}^{0} E(\left\|\nabla^{\pm}_{\omega} \chi_{\{f>t\}}\right\|_p)dt \\ &= \int_0^{+\infty} E(\left\|\nabla^{\pm}_{\omega} \chi_{\{f>t\}}\right\|_p)dt + \int_{-\infty}^{0} E(\left\|\nabla^{\pm}_{\omega} (-\chi_{\{f\le t\}})\right\|_p)dt \\ &\ge \lambda^{-1} \int_0^{\infty} E[g_1 \cdot \chi_{\{f>t\}}]dt + \lambda^{-1} \cdot \int_{-\infty}^{0} E\left(\chi_{\{f\le t\}} g_2\right) dt \\ &= \lambda^{-1} E(g_1 f^+) + \lambda^{-1} \cdot E(f^- g_2). \end{aligned}$$

We get the desired inequality by taking the supremum over all function $g_1, g_2 \in \mathcal{G}$. □

5. Discrete mean curvature flow on graphs.

5.1. Mean curvature on graphs. We first introduce a class of mean curvatures on graphs based on the definition of the nonlocal perimeters on graphs defined above. As in the nonlocal continuum case [14], we define the mean curvature as the first variation of the perimeter. We denote by $\delta(u)$ the degree of a vertex $u \in V$ which is given by $\delta(u) = \sum_{v\sim u} \sqrt{\omega_{uv}}$.

DEFINITION 5.1. *Let $\mathcal{A} \subset V$, and $u_0 \in V$. We define the upwind and downwind mean curvature as follow:*

$$\kappa^{+}_{\omega,1}(u_0,\mathcal{A}) \stackrel{\text{def}}{=} \frac{\mathrm{Per}^{+}_{\omega,1}(\mathcal{A}\cup\{u_0\}) - \mathrm{Per}^{+}_{\omega,1}(\mathcal{A})}{\delta(u_0)},$$

$$\kappa^{-}_{\omega,1}(u_0,\mathcal{A}) \stackrel{\text{def}}{=} \frac{\mathrm{Per}^{-}_{\omega,1}(\mathcal{A}) - \mathrm{Per}^{-}_{\omega,1}(\mathcal{A}\setminus\{u_0\})}{\delta(u_0)}.$$

Finally, we define then the mean curvature for $u_0 \in V$ as:

$$\kappa_{\omega,1}(u_0,\mathcal{A}) \stackrel{\text{def}}{=} \begin{cases} \kappa^{+}_{\omega,1}(u_0,\mathcal{A}), & \text{if } u_0 \in \mathcal{A}^c, \\ \kappa^{-}_{\omega,1}(u_0,\mathcal{A}), & \text{if } u_0 \in \mathcal{A}. \end{cases}$$

Observe that by a simple development of the definition of the perimeters, we show that

$$\mathrm{Per}^{+}_{\omega,1}(\mathcal{A}\cup\{u_0\}) - \mathrm{Per}^{+}_{\omega,1}(\mathcal{A}) = \begin{cases} \sum_{v\in\mathcal{A}^c}\sqrt{\omega_{u_0v}} - \sum_{v\in\mathcal{A}}\sqrt{\omega_{u_0v}}, & \text{if } u_0 \in \mathcal{A}^c, \\ 0, \quad \text{if } u_0 \in \mathcal{A}, \end{cases}$$

and

$$\mathrm{Per}^{-}_{\omega,1}(\mathcal{A}) - \mathrm{Per}^{-}_{\omega,1}(\mathcal{A}\setminus\{u_0\}) = \begin{cases} \sum_{v\in\mathcal{A}^c}\sqrt{\omega_{u_0v}} - \sum_{v\in\mathcal{A}}\sqrt{\omega_{u_0v}}, & \text{if } u_0 \in \mathcal{A}, \\ 0, \quad \text{if } u_0 \in \mathcal{A}^c. \end{cases}$$

Therefore, one gets an explicit formula of the discrete mean curvature.

PROPOSITION 5.1. *For all $\mathcal{A} \subset V$ and all $u_0 \in V$, we have:*

$$\begin{aligned} \kappa_{\omega,1}(u_0,\mathcal{A}) &= \frac{\sum_{v\in\mathcal{A}^c}\sqrt{\omega_{u_0v}} - \sum_{v\in\mathcal{A}}\sqrt{\omega_{u_0v}}}{\delta(u_0)} \\ &= -\frac{\sum_{v\in V}\sqrt{\omega_{u_0v}}(\chi_{\mathcal{A}} - \chi_{\mathcal{A}^c})}{\delta(u_0)}. \end{aligned} \tag{5.1}$$

REMARK 5.1. *(i) We can interpreted the formula (5.1) as a discrete version of the nonlocal J-mean curvature introduced in [34, Definition 3.2], which is given by*

$$H^{J}_{\partial E}(\boldsymbol{x}) \stackrel{\text{def}}{=} -\int_{\mathbb{R}^n} J(\boldsymbol{x}-\boldsymbol{y})(\chi_E(\boldsymbol{y}) - \chi_E(\boldsymbol{x}))d\boldsymbol{y}, \qquad x \in \mathbb{R}^n,$$

where $E \subset \mathbb{R}^n$ measurable set and J is a nonnegative radial measurable function in $L^1(\mathbb{R}^n)$.

(ii) Based on the equation (5.1), we can extend the notion of the mean curvature to any function f on graphs by considering its level sets. Indeed, let $f : V \to \mathbb{R}$ and $u \in V$. The mean curvature $\kappa_{\omega,1}$ (we keep the same notion) of f at u on a graph is defined as

$$\begin{aligned} \kappa_{\omega,1}(u,f) &\stackrel{\text{def}}{=} \kappa_{\omega,1}(u,\{f \geq f(u)\}) \\ &= \frac{\sum_{v\in\{f\geq f(u)\}}\sqrt{\omega_{uv}} - \sum_{v\in\{f<f(u)\}}\sqrt{\omega_{uv}}}{\delta(u)} \\ &= \frac{\sum_{v\in V}\sqrt{\omega_{u_0v}}\,\mathrm{sign}(f(v)-f(u))}{\delta(u)}, \end{aligned}$$

where

$$\operatorname{sign}(r) = \begin{cases} 1, & \text{if } r \geq 0, \\ -1, & \text{if } r < 0. \end{cases}$$

(iii) In the continuum (local) setting, the mean curvature, for a given smooth hypersurface $\Gamma \subset \mathbb{R}^N$, at a point $\boldsymbol{x}$ of Γ is given by the following formula

$$\kappa(\boldsymbol{x}) = -\operatorname{div}(n_{\boldsymbol{x}}), \tag{5.2}$$

where $n_{\boldsymbol{x}}$, $\boldsymbol{x} \in \Gamma$, is the unit normal vector field.
As in the continuous case, we are going to expose a discrete version of (5.2) on graphs, introduced in [48]. Let $G = (V, E, \omega)$ be a weighted graph. For a nonempty set $\mathcal{A} \subset V$, the analogue of (5.2) on graph is given as follow:

$$\kappa^{loc}_{\omega,1}(u, \mathcal{A}) = \operatorname{div}_w(n_{\mathcal{A}})(u) = \begin{cases} \sum_{v \in \mathcal{A}^c} \sqrt{\omega_{uv}}, & \text{if } u \in \mathcal{A}, \\ -\sum_{v \in \mathcal{A}} \sqrt{\omega_{uv}}, & \text{if } u \in \mathcal{A}^c, \end{cases} \tag{5.3}$$

where $n_{\mathcal{A}}$ is the discrete normal vector which is defined as

$$n_{\mathcal{A}}(u, v) = \begin{cases} 1 & \text{if } u \sim v \text{ and } (u, v) \in \mathcal{A} \times \mathcal{A}^c, \\ -1 & \text{if } u \sim v \text{ and } (u, v) \in \mathcal{A}^c \times \mathcal{A}, \\ 0 & \text{else.} \end{cases}$$

The formula given in [48] of the mean curvature is relatively different from this one, this difference returns to the definition of divergences considered. Observe that, the sign of the mean curvature, given by (5.3), depends only on the side that contains the vertex u and not on the weights function, while it is not in the case of the mean curvature considered in Definition 5.1, which makes a difference in the study of the data processing especially the nonlocal ones. In the rest of this work, we adopt Definition 5.1 for the discrete mean curvature.

6. Level set formulation of mean curvature flows on graphs. Based in a discretization of the gradients and curvatures on a general domain, graph, we can adapt a large PDEs models on graphs involving mean curvature or variants of mean curvature. In this section we consider two general models used extensively to solve several tasks in image processing and computer vision. The level power mean curvature flows for image denoising, enhancement or simplification and the PDEs level set active contours for image segmentation and object detection. We will show that the transposition of these models on graphs leads to partial differences equations with coefficients that depend on data and their applications are naturally extend to the processing of any data and for data classification.

6.1. Level set power mean curvature flow on Euclidean domain. The level set method for front propagation has been used with great success in both pure and applications and in different applications in image processing and computer vision. The level set approach was first proposed by Osher and Sethian [42] to model evolving fronts with curvature, see also the recent works [38, 10]. The level set is used to analyse its subsequent motion under a normal velocity $c(\boldsymbol{x}, t)$. The idea is to represent the evolving front as a level set of a function $\phi(\boldsymbol{x}, t)$ for $\boldsymbol{x} \in \mathbb{R}^n$ and t

is the time. The initial front is given by $\Gamma_0 = \{\boldsymbol{x} : \ \phi(\boldsymbol{x}, 0) = 0 = \phi_0\}$, where ϕ_0 is a smooth function defined on $\mathbb{R}^n$, and the evolving front is described for all later time as $\Gamma_t = \{\boldsymbol{x} : \ \phi(\boldsymbol{x}, t) = 0\}$. The evolving front is governed by the following equation:

$$\begin{cases} \frac{\partial \phi}{\partial t}(\boldsymbol{x}, t) & = c(\boldsymbol{x}, t) \big\| \nabla \phi(\boldsymbol{x}, t) \big\|_2, \quad (\boldsymbol{x}, t) \in \mathbb{R}^n \times (0, T) \\ \phi(\boldsymbol{x}, 0) & = \phi_0(\boldsymbol{x}), \quad \boldsymbol{x} \in \mathbb{R}^n. \end{cases} \tag{6.1}$$

For $c(\boldsymbol{x}, t) = \big|\kappa(\boldsymbol{x}, t)\big|^{\alpha - 1} \kappa(\boldsymbol{x}, t)$ where κ presents the usual mean curvature, we have the level set power mean curvature equation, [41]. In particular, when $\alpha = 1$ this equation corresponds to the mean curvature flow filter which finds important applications in image processing [42], while the case when $\alpha \to 0$, we obtain so called conditional erosion/dilatation based on the sign of the mean curvature used in mathematical morphology. A variant for positive/negative curvature flows are used in [33] for image enhancement in addition to noise removal.

In the case, where ϕ_0 is an implicit representation of a front (surface), we get the active contour/snake model which is one of the most successful variational models in image segmentation. It consists of evolving a contour in images toward the boundaries of objects. Its success is based on strong mathematical properties and efficient numerical schemes via the level sets method. A general formula of this method can be written as follows

$$\begin{cases} \frac{\partial \phi}{\partial t}(\boldsymbol{x}, t) & = \left(\alpha \operatorname{div} \left(\frac{\nabla \phi(\boldsymbol{x}, t)}{\big\| \nabla \phi(\boldsymbol{x}, t) \big\|_2} \right) + \beta \, F(I, \phi(\boldsymbol{x}, t)) \right) \big\| \nabla \phi(\boldsymbol{x}, t) \big\|_2, \\ \phi(\boldsymbol{x}, 0) & = \phi_0(\boldsymbol{x}), \end{cases} \tag{6.2}$$

where $I : \Omega \to \mathbb{R}$ is the initial image, $\alpha, \beta \in \mathbb{R}$ and F is a halting function of the active contour model.

In particular, Chan-Vese model for active contours [16, 49] is a powerful and flexible method which detects objects whose boundaries are not necessarily detected by the gradient. This model is based on an energy minimization problem, which can be reformulated in the level set formulation, leading to an easier way to solve the problem. Chan-Vese model has achieved well performance in image segmentation task due to its ability of obtaining a larger convergence range and handling topological changes naturally.

$$\begin{cases} \frac{\partial \phi}{\partial t}(\boldsymbol{x}, t) & = \left(\alpha \operatorname{div} \left(\frac{\nabla \phi(\boldsymbol{x}, t)}{\big\| \nabla \phi(\boldsymbol{x}, t) \big\|_2} \right) - \lambda_1 (I - c_1)^2 + \lambda_2 (I - c_2)^2 \right) \big\| \nabla \phi(\boldsymbol{x}, t) \big\|_2, \\ \phi(\boldsymbol{x}, 0) & = \phi_0(\boldsymbol{x}). \end{cases} \tag{6.3}$$

where $\alpha, \ \lambda_1, \ \lambda_2 > 0$ are the fitting parameters, I corresponds to the initial image, ϕ_0 is a smooth function, c_1 the average of I on $\phi(\boldsymbol{x}, t) \geq 0$, and c_1 the average of I on $\phi(\boldsymbol{x}, t) \leq 0$.

6.2. Transcription of power mean curvature flow on graphs. We are interested in translating on graphs two PDEs models involving mean curvature. Let $G = (V, E, \omega)$ be a weighted graph, based on the definition of discrete gradient and

the boundary set which are given above, our formulation for the level set power mean curvature equation (6.1) on graphs can be expressed as follows:

$$\begin{cases} \frac{\partial \phi}{\partial t}(u,t) &= \left(\left|\kappa_\omega(\phi(u,t))\right|^{\alpha-1}\kappa_\omega(\phi(u,t))\right)^+ \left\|\nabla_\omega^+\phi(u,t)\right\|_p \\ &\quad - \left(\left|\kappa_\omega(\phi(u,t))\right|^{\alpha-1}\kappa_\omega(\phi(u,t))\right)^- \left\|\nabla_\omega^-\phi(u,t)\right\|_p, \\ \phi(u,0) &= \phi_0(u), \end{cases} \tag{6.4}$$

where $\phi_0(\cdot,t) \in \mathcal{H}(V)$, $\alpha \in [0,1]$, $p \in [1,+\infty]$ and

$$\kappa_\omega(\phi(u,t)) = \kappa_{\omega,1}\left(u, \{y \mid \ \phi(v,t) \geq \phi(u,t)\}\right).$$

We use the forward/explicit Euler scheme in the time to approximate the above problem, for that let $0 < t_1 < t_2 < \cdots < t_\ell = T$ be an equispaced partition of $[0,T]$, $T > 0$. i.e. $t_i = \frac{i}{\ell}T,\ i \in [\ell]$.

$$\frac{\partial \phi}{\partial t}(u,t) = \frac{\phi^{i+1}(u) - \phi^i(u)}{\Delta t},$$

where $\phi^i(u) = \phi(u, i\Delta t)$ with $\Delta t = \frac{T}{\ell}$ and the equation (6.4) can be rewritten as the following iterative equation:

$$\begin{aligned} \phi^{i+1}(u) - \phi^i(u) = \Delta t\Bigg(&\left(\left|\kappa_\omega(\phi^i(u))\right|^{\alpha-1}\kappa_\omega(\phi^i(u))\right)^+ \left\|\nabla_\omega^+\phi^i(u)\right\|_p \\ &- \left(\left|\kappa_\omega(\phi^i(u))\right|^{\alpha-1}\kappa_\omega(\phi^i(u))\right)^- \left\|\nabla_\omega^-\phi^i(u)\right\|_p\Bigg). \end{aligned}$$

In particular, for $\alpha = 1$ the equation (6.4) can rewritten as the following iterative equation:

$$\begin{cases} \phi^{i+1}(u) &= \phi^i(u) + \Delta t\Bigg(\left(\kappa_\omega(\phi^i(u))\right)^+ \left\|\nabla_\omega^+\phi^i(u)\right\|_p \\ &\quad - \left(\kappa_\omega(\phi^i(u))\right)^- \left\|\nabla_\omega^-\phi^i(u)\right\|_p\Bigg), \\ \phi^0(u) &= \phi_0(u). \end{cases} \tag{6.5}$$

When $p = \infty$, we across the scheme considered in [22, Section 3.3]. Now, let us consider the case that when $\alpha \to 0$ and $p = \infty$. Similarly by using the explicit Euler method as above, one gets the following iterative equation :

$$\begin{cases} \phi^{i+1}(u) &= \phi^i(u) + \Delta t\Bigg(\operatorname{sign}\left(\kappa_\omega(\phi^i(u))\right) \left\|\nabla_\omega^+\phi^i(u)\right\|_\infty \\ &\quad + \operatorname{sign}\left(\kappa_\omega(\phi^i(u))\right) \left\|\nabla_\omega^-\phi^i(u)\right\|_\infty\Bigg), \\ \phi^0(u) &= \phi_0(u). \end{cases} \tag{6.6}$$

In the case where $\Delta t = 1$, this previous equation can be interpreted as

$$\phi^{i+1}(u) = \begin{cases} \phi^i(u) + \left\|\nabla_\omega^+\phi^i(u)\right\|_\infty, & \text{if } \kappa_\omega(\phi^i(u)) \geq 0, \\ \phi^i(u) - \left\|\nabla_\omega^-\phi^i(u)\right\|_\infty, & \text{if } \kappa_\omega(\phi^i(u)) < 0. \end{cases} \tag{6.7}$$

6.3. Transcription of the active contour on graphs. In this section, we present a transcription of geometric PDEs on weighted graphs of arbitrary topology. A front evolving on G is defined as a subset $\mathcal{A}_0 \subset V$, and is implicitly represented by a level set function $\phi_0 = \chi_{\mathcal{A}_0} - \chi_{\mathcal{A}_0^c}$. In other word ϕ_0 equal 1 in $\mathcal{A}_0$ and -1 on its complementary. From the general equation (6.1) transposed on graph, the front propagation can be expressed in general by

$$\begin{cases} \frac{\partial \phi}{\partial t}(u,t) & = c(u,t) \cdot \left\| \nabla_\omega \phi(u,t) \right\|_p \quad (u,t) \in V \times [0,T) \\ \phi(u,0) & = \phi_0(u), \end{cases} \tag{6.8}$$

with $c(\cdot,t) \in \mathcal{H}(V)$. Based on the previous definition of discrete dilation and erosion on graphs, the front propagation can be expressed as a morphological process with the following sum of dilation and erosion.

$$\begin{cases} \frac{\partial \phi}{\partial t}(u,t) & = (c(u,t))^+ \cdot \left\| \nabla_\omega^+ \phi(u,t) \right\|_p - (c(u,t))^- \cdot \left\| \nabla_\omega^- \phi(u,t) \right\|_p \\ \phi(u,0) & = \phi_0(u). \end{cases}$$

To solve this dilation and erosion process, on the contrary to the PDEs case, no spatial discretization is needed thanks to derivatives directly expressed in a discrete form. Then, the general iterative scheme to compute ϕ at time $t+1$ for all $u \in V$ is given by:

$$\phi^{i+1}(u) = \phi^i(u) + \Delta t \left((c(u,t))^+ \left\| (\nabla_\omega^+ \phi^i)(u) \right\| - (c(u,t))^- \left\| (\nabla_\omega^- \phi^i)(u) \right\| \right).$$

At each time $i+1$, the new value at a vertex u only depends on its value at time i and the existing values in its neighborhood. This equation can be split in two independent equations, in function of the sign of $c(\cdot,\cdot)$:

$$\phi^{i+1}(u) = \begin{cases} \phi^i(u) + \Delta t (c(u,t)) \left\| (\nabla_\omega^+ \phi^i)(u) \right\|, & \text{if } c(u,t) > 0, \\ \phi^i(u) + \Delta t (c(u,t)) \left\| (\nabla_\omega^- \phi^i)(u) \right\|, & \text{if } c(u,t) < 0, \end{cases}$$

Such decomposition of the process in two independent equations for erosion and dilation processes enhances the computation of the solution because one only has to compute one morphological gradient at each iteration, for a given vertex. Moreover, one can remark that at initialization both two gradients are zero everywhere, except for vertices which lies in the inner and outer boundaries of $\mathcal{A}_0$. Then, the set of vertices to be updated at each iteration can be restricted to two inner and outer narrow bands, initialized respectively with $\partial^- \mathcal{A}_0$ and $\partial^+ \mathcal{A}_0$ and updated over time with neighbours of vertices already in. The narrow bands growth follows the fronts evolution and to avoid them to become too large, the narrow bands are reinitialized periodically. Thus, each τ iterations,which correspond to a step k, the front is given by the set $\mathcal{A}_k = \left\{ u \in V : \phi^{k\tau}(u) > 0 \right\}$ and the associated level set function is also reinitialized as $\phi_k(u) = \mathcal{U}_k = \chi_{\mathcal{A}_k}(u) - \chi_{\mathcal{A}_k^c}(u)$. Then, the inner and outer narrow bands are respectively reinitialized as $\partial^- \mathcal{A}_k$ and $\partial^+ \mathcal{A}_k$.

REMARK 6.1. *Using previous definitions of morphological evolution equations, one can formulate the same relation and obtain a PdEs-based version of the Eikonal equation, defined on weighted graphs of arbitrary topology. Indeed, let $c = 1$ and $\phi(\cdot,t) = t - \varphi(\cdot)$ on the whole domain V, with $\varphi \in \mathcal{H}(V)$. We obtain a discrete*

adaptation of the Eikonal equation on graph, which describes a morphological erosion process, and defined as

$$\begin{cases} \left\| \left(\nabla_\omega^- \varphi\right)(u) \right\| = 1, & u \in V_0, \\ \varphi(u) = 0, & u \in V \setminus V_0, \end{cases} \tag{6.9}$$

where $V_0 \subset V$. Numerical schemes and algorithms to solve such equation have provided in [18]. These shemes allow to compute weighted geodesic distances, see [18, Section 5.2].

7. Numerical experiments. In this section, we present our numerical experiments to illustrate the potentialities of our formulations of the level set power mean curvature equation, through two models: power mean curvature flows and Chan-Vese model for active contour. These allow us to process both images and $3D$-point clouds. Different graph structures and weight functions are also used to show the flexibility of our approach.

7.1. Weighted graph construction. There exist several popular methods to transform discrete data $\{u_1, \cdots, u_n\}$ into a weighted graph structure. Considering a set of vertices V such that the data are embedded by functions of $\mathcal{H}(V)$, the construction of such a graph consists in modeling the neighborhood relationships between the data through the definition of a set of edges E and using a pairwise distance measure $\mu : V \times V \to \mathbb{R}^+$. In the particular case of images, graph construction methods based on geometric neighborhoods are particularly well-adapted to represent the geometry of the space, as well as the geometry of the function defined on that space. We distinguish the following types of graphs:

- *Grid graphs*, which are the most natural structures to describe an image with a graph. Each pixel is connected by an edge to its adjacent pixels. Classical grid graphs are 4-adjacency grid graphs and 8-adjacency grid graphs. Larger adjacency can be used to obtain nonlocal grid graphs.
- *Region adjacency graphs* (RAGs), which provide very useful ways of describing the structure of a picture: vertices represent regions and edges represent region adjacency relationship.
- *k-nearest neighborhood graphs* (k-NNGs), where each vertex u is connected with its k-nearest neighbors according to the distance measure μ. Such construction implies building a directed graph as the neighborhood relationship is not symmetric. Nevertheless, an undirected graph can be obtained by adding an edge between two vertices u and v if u is among the k-nearest neighbors of v or if v is among the k-nearest neighbors of u.
- *k-extended RAGs* (k-ERAGs), which are RAGs extended by a k-NNG. Each vertex is connected to adjacent regions vertices and to its k most similar vertices of V.

The similarity between two vertices is computed with respect to an appropriate measure $s : E \to \mathbb{R}^+$, which satisfies

$$\omega_{uv} = \begin{cases} s(u,v), & \text{if } (u,v) \in E, \\ 0, & \text{otherwise.} \end{cases}$$

Examples for common similarity functions are as follows:

- $s_0(u,v) = 1$;
- $s_1(u,v) = \exp(-d(u,v)/\sigma^2)$, with $\sigma > 0$, where d is a metric controlling the similarity between edges, and σ is a scale parameter.

- For patch-based methods, the similarity function is

$$s_2(u,v) = \exp(-\mu(u,v)^2/\sigma^2), \text{ with } \sigma > 0,$$

where now $\mu(u,v) = \left\|\mathcal{P}(u) - \mathcal{P}(v)\right\|_2$, and $\mathcal{P} : u \in V \mapsto \mathcal{P}(u) \in \mathbb{R}^m$ is the patch extraction operator at u. For each node/vertex u, $\mathcal{P}(u)$ is an m-dimensional real vector containing, e.g., spatial coordinates, intensities, etc., of the neighbours of u. This definition of patches is valid only for grid-graphs and cannot be considered for arbitrary graphs. To compute the patch on a $3D$ point cloud, the reader is referred to [32].

Several choices can be considered as feature vectors computed from the given data, depending on the nature of the features to be used for graph processing. In the context of image processing one can use the simple grayscale or color feature vector F_u, or a patch feature vector $F_u^\tau = \bigcup_{v\in\mathcal{W}^\tau(u)} F_v$ (i.e., the set of values F_v, where v is in a square window $\mathcal{W}^\tau(u)$ of size $(2\tau+1)\times(2\tau+1)$ centered at a vertex pixel u) incorporating nonlocal features such as texture.

7.2. Mean curvature flow. This paragraph illustrates the mean curvature flow filtering real image data, defined both on two-dimensional regular grid and three-dimensional point cloud. Figure 1 presents filtering results of an image using the formulation of the mean curvature flow (6.4), with $p = 2$ and different graph construction (local and nonlocal). We used two types of local graphs, both are built as a usual 4-adjacency grid graph where $\omega = s_0$ for the first one, while $\omega = s_1$ for the second (pixels are characterized by their color feature vectors). The nonlocal graph is built using a k-NNG in a 11×11 neighborhood window and each pixel is characterized by a 5×5 patch of color feature vectors (the weight function holds similarity between patches, with $\omega = s_2$).

Figure 2 presents filtering results obtaining of $3D$-point cloud using the same formulation. In this example, we applied our formulation using two graphs. Both built from the same $3D$-points clouds using k-NNGs, with $k = 8$ and $\omega = s_0$ for the first one, which their correspond result is given by (b). For the second graph, we took $k = 10$ and $\omega = \exp(-d(\phi_0(u),\phi_0(v))/10^2)$, which their correspond result is given by (c), where ϕ_0 (RGB color vectors) represents the initial datum and d is the Euclidean distance between $\phi_0(u)$ and $\phi_0(v)$.

7.3. Active contour model on graphs.

Image segmentation using local and non-local graph. In this paragraph, we illustrate the behaviour of the Chan-Vese model (6.3). An advantage of our graph-based formulation is that the proposed formula can be applied to any graph, and therefore any graph representing images. To illustrate such an adaptive behaviour, we propose to use other image structures for image segmentation. Figure 3 and Figure 4 present results segmentation, with local and nonlocal graphs, respectively. The local graph is built as a usual 4-adjacency grid graph where each pixel is characterized by its color feature vector. The nonlocal one is built using a k-NNG in a 11×11 neighborhood window and each pixel is characterized by a 5×5 patch of color feature vectors.

Image segmentation using region adjacency graph. The following example will illustrate graph-based versions of eikonal equation and active contours, with our formulation of PDEs level sets on graphs, in a unique application. For this example, we adapt Chan and Vese active contour model (6.3), on weighted graphs. The active contour evolution is performed on a reduced version of the initial image, a region adjacency graph (RAG), obtained from a superpixel decomposition. Such decomposition

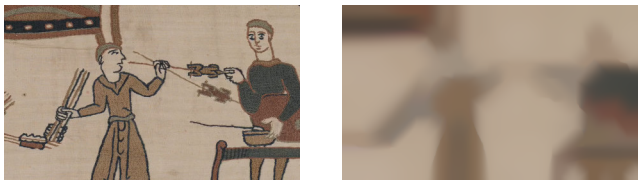

(a) Original image (b) $\omega = s_0$

(c) $\omega = s_1$ (d) $\omega = s_2$

Fig. 1: Colored image filtering with mean curvature flows.(a) Original image.(b) and (c) present results with 4-adjacency grid graph, where $\omega = s_0$ and $\omega = s_1$, respectively. (d) presents result with k-NNG. See text for more detail.

(a) Original image

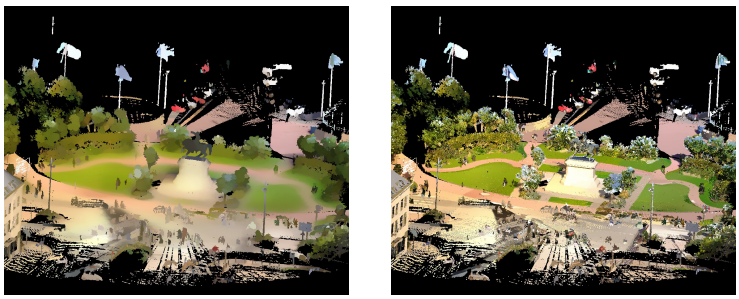

(b) $\omega = s_0$ (c) $\omega = s_1$

Fig. 2: Colored point cloud filtering with mean curvature flows. (a) Original image. (b) presents results obtained using local k-NNGs ($k = 8$ and $\omega = 1$). (c) presents results under the same configuration but with different similarity function (ω =colour, which depends on the colour similarity between different $3D$-points), obtained using 20-NNGs.

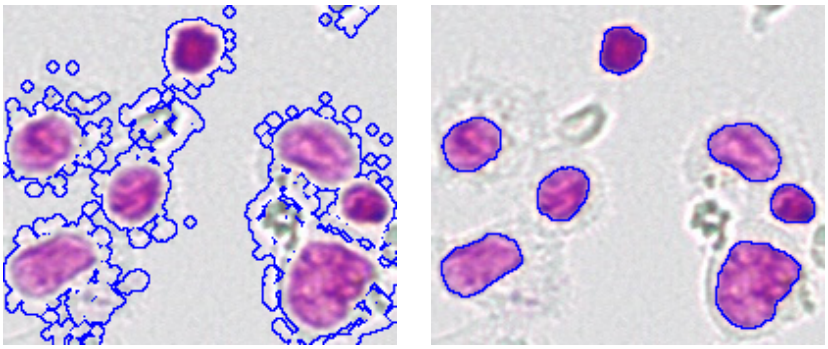

(a) Initial contour (b) Final contour

Fig. 3: Illustration of Chan-Vese segmentation with two phases, using a local 4-adjacency grid graph where each pixel is characterized by it's color feature vector.

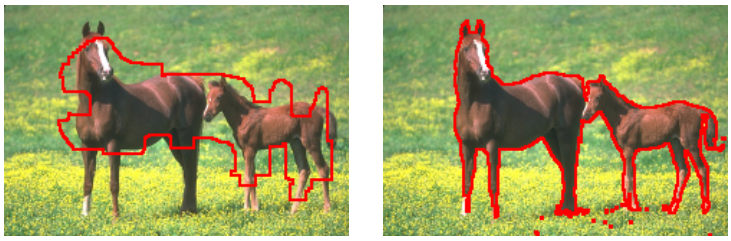

(a) Initial contour (b) Final contour

Fig. 4: Illustration of Chan-Vese segmentation with two phases, using k-NNG. See text for more detail.

is performed using a regular-grid of seeds, which are dilated on the image 4-adjacency-grid graph using the PdEs based version of the eikonal equation (16). The resulting region map is then transformed in a second graph (the RAG) where each node is associated with a superpixel and edges represent the adjacency between superpixels. The two weight functions are computed from pixels intensity, respectively regions mean intensity. A detailed description of the method can be found in [19]. One can remark that due to its construction the second graph is irregular. Then, the active contour evolution is performed on this second graph, using our formulation of active contours on weighted graphs. Finally, the contour at convergence of the algorithm is transposed from the graph to the region map and then to the original image. Figure 5 presents each steps of the entire process.

Data clustering. In this experiment, we show that our level set active contour method can also be used for data clustering purposes, when data are represented as points cloud. To do so, we have selected a small part of the MNIST dataset [31]. This dataset is composed of handwritten digits, stored as small images. The subset we chose is composed of 2 classes : 0's and 1's. For the illustration we picked 200 elements of each. We constructed a k-nearest neighbors on this dataset, with $k = 5$. To compute the distance between two images, we used the two-sided tangent distance

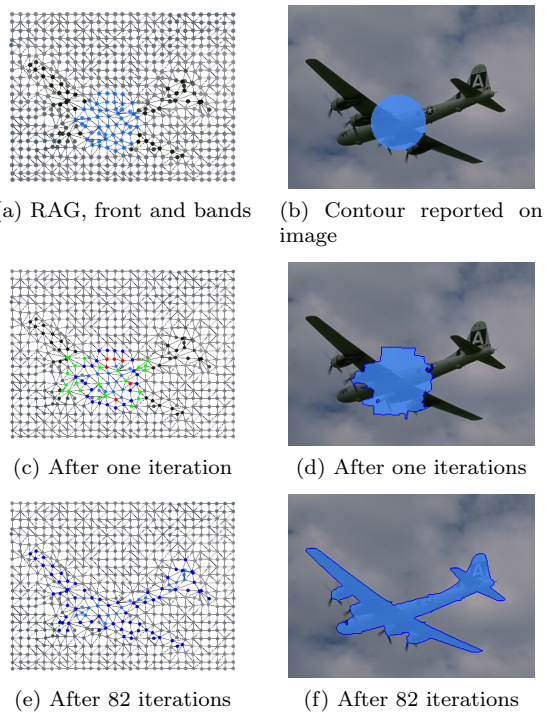

(a) RAG, front and bands (b) Contour reported on image

(c) After one iteration (d) After one iterations

(e) After 82 iterations (f) After 82 iterations

Fig. 5: Illustration of active contour on a region adjacency graph (RAG). The RAG is built from a superpixel decomposition of the initial image, where each region is connected to its adjacent regions. The weight and velocity functions are computed from the mean color inside regions. Left column shows the RAG, with the front in blue and candidate bands in red (inner) an green (outer). Right column shows the initial image with the front transposed from the RAG (using the superpixels boundaries).

[30], an extension of the tangent distance used in [44], especially well suited for this dataset. In this experiment, we begin from an initial random partition that we refine using our approach. To do so, we initialize both fronts Γ^1 (in blue) and Γ^2 (in red) as two random sets of digits and let them move under the effect of the velocity function with an additional curvature term. We use the discrete mean curvature on graphs (See Definition 5.1). The graph and several iterations are presented in Figure 6

High dimensional semi-supervised data classification. Finally, we have tested the performance of our proposed framework when applied to semi-supervised classification on three standard databases from the literature: MNIST [31], OPTDIGITS [3], and PENDIGITS [2]. We compare two kinds of velocities. The first one is the active contour on the graph-based curvature. We denote it as AC. The second one is propagation using the evolution eikonal equation but constant in time and based on the characteristic of graph vertices. We denote it as EE. For these databases we merged both the training and the test sets (as performed in [6]), resulting in datasets of 70000 instances, 5620 instances, and 10992 instances, for MNIST, OPTDIGITS, and PENDIGITS, respectively. In our tests, we propose also, to refine the classification results of EE with AC algorithm (i.e., EE is used as seeds for AC), and we denote it as EE + AC. In Table 1, we expose a comparainson between these methodes,

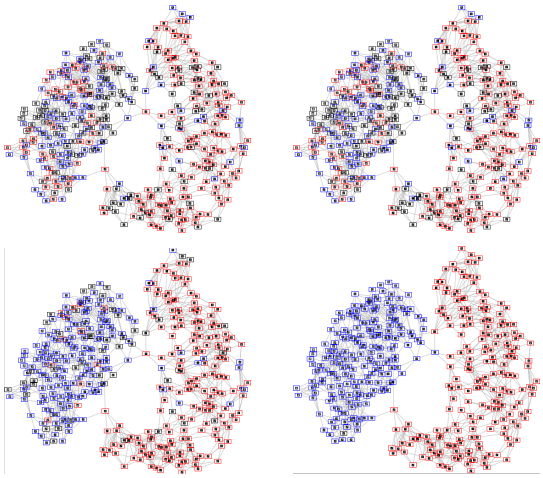

Fig. 6: Illustration of the algorithm for active contours on points cloud data for clustering. The graph is built from a small subset of the MNIST database, as a k-NNG (with $k = 5$). The weight function is computed using two-sided tangent distance and the velocity is defined according to graph-based curvature and intra an inter class similarities. Each cluster is represented by a front, randomly initialized. The clustering is performed by fronts motion using evolution eikonal equation.

where we vary the amount of initial seeds from 1% to 10%, and compute the average classification rate over 10 runs of each algorithm.

seeds	datasets	EE	AC	EE+AC
1%	MNIST	97.45%	98.20%	98.24%
	OPTDIGITS	95.22%	96.82%	97.10%
	PENDIGITS	95.75%	95.71%	96.25%
2%	MNIST	97.64%	98.24%	98.29%
	OPTDIGITS	97.41%	97.88%	97.92%
	PENDIGITS	97.38%	97.06%	98.56%
5%	MNIST	97.95%	98.33%	98.37%
	OPTDIGITS	98.09%	98.38%	98.35%
	PENDIGITS	98.25%	98.30%	98.56%
10%	MNIST	98.19%	98.39%	98.45%
	OPTDIGITS	98.41%	98.64%	98.51%
	PENDIGITS	98.94%	98.92%	99.10%

Table 1: Classification rates on the three datasets.

Acknowledgment. The first author has been supported by MIDIPATH project. The second author has been supported by the French Research Agency through the SUMUM project (ANR-17-CE38-0004).

REFERENCES

[1] N. Abatangelo and E. Valdinoci, *A notion of nonlocal curvature*, Numerical Functional Analysis and Optimization, 35 (2014), pp. 793–815.

[2] F. Alimoğlu and E. Alpaydin, *Combining multiple representations for pen-based handwritten digit recognition*, Turkish Journal of Electrical Engineering & Computer Sciences, 9 (2001), pp. 1–12.

[3] E. Alpaydin and C. Kaynak, *Optical recognition of handwritten digits, uci machine learning repository*, 1998.

[4] L. Ambrosio, G. De Philippis, and L. Martinazzi, *Gamma-convergence of nonlocal perimeter functionals*, Manuscripta Mathematica, 134 (2011), pp. 377–403.

[5] J. Bourgan, H. Brezis, and P. Mironescu, *Another look at sobolev spaces*, in Optimal control and partial differential equation. Conference, 2001, pp. 439–455.

[6] X. Bresson, T. Laurent, D. Uminsky, and J. H. Von Brecht, *Multiclass total variation clustering*, arXiv preprint arXiv:1306.1185, (2013).

[7] H. Brezis, *How to recognize constant functions. connections with sobolev spaces*, Russian Mathematical Surveys, 57 (2002), p. 693.

[8] B. Buet, J.-M. Mirebeau, Y. van Gennip, F. Desquilbet, J. Dreo, F. Barbaresco, G. P. Leonardi, S. Masnou, and C.-B. Schönlieb, *Partial differential equations and variational methods for geometric processing of images*, The SMAI journal of computational mathematics, 5 (2019), pp. 109–128.

[9] T. Bühler and M. Hein, *Spectral clustering based on the graph p-Laplacian*, in Proceedings of the 26th Annual International Conference on Machine Learning, ICML '09, New York, NY, USA, 2009, ACM, pp. 81–88, doi:10.1145/1553374.1553385, http://doi.acm.org/10.1145/1553374.1553385.

[10] M. Burger, A. C. Mennucci, S. Osher, and M. Rumpf, *Level Set and PDE Based Reconstruction Methods in Imaging: Cetraro, Italy 2008, Editors: Martin Burger, Stanley Osher*, vol. 2090, Springer, 2013.

[11] L. CAFFARELLI, J.-M. ROQUEJOFFRE, and O. SAVIN, *Nonlocal minimal surfaces*, Communications on pure and applied mathematics, 63 (2010), pp. 1111–1144.

[12] L. Caffarelli and E. Valdinoci, *Uniform estimates and limiting arguments for nonlocal minimal surfaces*, Calculus of Variations and Partial Differential Equations, 41 (2011), pp. 203–240.

[13] J. Calder, *The game theoretic p-laplacian and semi-supervised learning with few labels*, Nonlinearity, 32 (2018), p. 301.

[14] A. Chambolle, M. Morini, and M. Ponsiglione, *Nonlocal curvature flows*, Archive for Rational Mechanics and Analysis, 218 (2015), pp. 1263–1329.

[15] A. Chambolle and T. Pock, *Approximating the total variation with finite differences or finite elements*, 2021.

[16] T. F. Chan and L. A. Vese, *Active contours without edges*, IEEE Transactions on image processing, 10 (2001), pp. 266–277.

[17] J. Dávila, *On an open question about functions of bounded variation*, Calculus of Variations and Partial Differential Equations, 15 (2002), pp. 519–527.

[18] X. Desquesnes, A. Elmoataz, and O. Lézoray, *Eikonal equation adaptation on weighted graphs: fast geometric diffusion process for local and non-local image and data processing*, Journal of Mathematical Imaging and Vision, 46 (2013), pp. 238–257.

[19] X. Desquesnes, A. Elmoataz, O. Lézoray, and V.-T. Ta, *Efficient algorithms for image and high dimensional data processing using eikonal equation on graphs*, in International Symposium on Visual Computing, Springer, 2010, pp. 647–658.

[20] A. El Alaoui, X. Cheng, A. Ramdas, M. J. Wainwright, and M. I. Jordan, *Asymptotic behavior of ℓ_p-based laplacian regularization in semi-supervised learning*, in Conference on Learning Theory, 2016, pp. 879–906.

[21] I. El Bouchairi, J. Fadili, and A. Elmoataz, *Continuum limit of p-laplacian evolution problems on graphs : L^q graphons and sparse graphs*, arXiv preprint arXiv:2010.08697. submitted to Numerische Mathematik., (2020).

[22] A. El Chakik, A. Elmoataz, and X. Desquesnes, *Mean curvature flow on graphs for image and manifold restoration and enhancement*, Signal processing, 105 (2014), pp. 449–463.

[23] A. Elmoataz, X. Desquesnes, and O. Lézoray, *Non-local morphological pdes and p-Laplacian equation on graphs with applications in image processing and machine learning*, IEEE Journal of Selected Topics in Signal Processing, 6 (2012), pp. 764–779.

[24] A. Elmoataz, X. Desquesnes, and M. Toutain, *On the game p-Laplacian on weighted graphs with applications in image processing and data clustering*, European Journal of Applied

Mathematics, 28 (2017), pp. 922–948.
[25] A. Elmoataz, O. Lezoray, and S. Bougleux, *Nonlocal discrete regularization on weighted graphs: a framework for image and manifold processing*, IEEE transactions on Image Processing, 17 (2008), pp. 1047–1060.
[26] A. Elmoataz, M. Toutain, and D. Tenbrinck, *On the p-Laplacian and ∞-Laplacian on graphs with applications in image and data processing*, SIAM Journal on Imaging Sciences, 8 (2015), pp. 2412–2451.
[27] L. J. Grady and J. R. Polimeni, *Discrete calculus: Applied analysis on graphs for computational science*, Springer Science & Business Media, 2010.
[28] Y. Hafiene, J. Fadili, and A. Elmoataz, *Nonlocal p-Laplacian evolution problems on graphs*, SIAM Journal on Numerical Analysis, 56 (2018), pp. 1064–1090.
[29] L. Hagen and A. B. Kahng, *New spectral methods for ratio cut partitioning and clustering*, IEEE transactions on computer-aided design of integrated circuits and systems, 11 (1992), pp. 1074–1085.
[30] D. Keysers, J. Dahmen, T. Theiner, and H. Ney, *Experiments with an extended tangent distance*, in Proceedings 15th International Conference on Pattern Recognition. ICPR-2000, vol. 2, IEEE, 2000, pp. 38–42.
[31] Y. LeCun and C. Cortes, *The mnist database of handwritten digits*, URL http://yann.lecun.com/exdb/mnist, (2010).
[32] F. Lozes, A. Elmoataz, and O. Lézoray, *Partial difference operators on weighted graphs for image processing on surfaces and point clouds*, IEEE Transactions on Image Processing, 23 (2014), pp. 3896–3909.
[33] R. Malladi and J. A. Sethian, *Image processing: Flows under min/max curvature and mean curvature*, Graphical models and image processing, 58 (1996), pp. 127–141.
[34] J. M. Mazón, J. D. Rossi, and J. Toledo, *Nonlocal perimeter, curvature and minimal surfaces for measurable sets*, Journal d'Analyse Mathématique, 138 (2019), pp. 235–279.
[35] J. M. Mazón, M. Solera, and J. Toledo, *The heat flow on metric random walk spaces*, Journal of Mathematical Analysis and Applications, 483 (2020), p. 123645.
[36] J. M. Mazón, M. Solera, and J. Toledo, *The total variation flow in metric random walk spaces*, Calculus of Variations and Partial Differential Equations, 59 (2020), pp. 1–64.
[37] D. B. Mumford and J. Shah, *Optimal approximations by piecewise smooth functions and associated variational problems*, Communications on pure and applied mathematics, (1989).
[38] S. Osher and R. Fedkiw, *Level set methods and dynamic implicit surfaces*, vol. 153, Springer Science & Business Media, 2006.
[39] Y. Peres and S. Sheffield, *Tug-of-war with noise: a game-theoretic view of the p-laplacian*, Duke Mathematical Journal, 145 (2008), pp. 91–120.
[40] L. I. Rudin, S. Osher, and E. Fatemi, *Nonlinear total variation based noise removal algorithms*, Physica D: nonlinear phenomena, 60 (1992), pp. 259–268.
[41] F. Schulze, *Evolution of convex hypersurfaces by powers of the mean curvature*, Mathematische Zeitschrift, 251 (2005), pp. 721–733.
[42] J. A. Sethian, *Level set methods and fast marching methods: evolving interfaces in computational geometry, fluid mechanics, computer vision, and materials science*, vol. 3, Cambridge university press, 1999.
[43] J. Shi and J. Malik, *Normalized cuts and image segmentation*, IEEE Transactions on pattern analysis and machine intelligence, 22 (2000), pp. 888–905.
[44] P. Y. Simard, Y. A. LeCun, J. S. Denker, and B. Victorri, *Transformation invariance in pattern recognition—tangent distance and tangent propagation*, in Neural networks: tricks of the trade, Springer, 1998, pp. 239–274.
[45] A. Szlam and X. Bresson, *Total variation, cheeger cuts*, in ICML, 2010.
[46] V.-T. Ta, A. Elmoataz, and O. Lézoray, *Nonlocal pdes-based morphology on weighted graphs for image and data processing*, IEEE transactions on Image Processing, 20 (2010), pp. 1504–1516.
[47] J.-P. Tillich, *Edge isoperimetric inequalities for product graphs*, Discrete Mathematics, 213 (2000), pp. 291–320.
[48] Y. Van Gennip, N. Guillen, B. Osting, and A. L. Bertozzi, *Mean curvature, threshold dynamics, and phase field theory on finite graphs*, Milan Journal of Mathematics, 82 (2014), pp. 3–65.
[49] L. A. Vese and T. F. Chan, *A multiphase level set framework for image segmentation using the mumford and shah model*, International journal of computer vision, 50 (2002), pp. 271–293.
[50] U. Von Luxburg, *A tutorial on spectral clustering*, Statistics and computing, 17 (2007), pp. 395–416.